International Research Journal of Engineering and Technology (IRJET) e-ISSN: 2395-0056
Volume: 05 Issue: 11 | Nov 2018 www.irjet.net p-ISSN: 2395-0072

Dynamic Properties of Cellular Lightweight Concrete

Anjali S[1], Anu V V[2]

[1]*UG student, Civil Department, Toc H Institute of Science and Technology*
[2]*Asst. Professor, Civil Department, Toc H Institute of Science and Technology*

Abstract - *Cellular lightweight concrete also known as foamed concrete, foamcrete or reduced density concrete is a cement-based slurry with a minimum of 20% foam entrained into mortar. They have been used widely in construction industry for over decades. They find applications in various forms due to their lightweight, thermal and sound insulation properties. They are eco-friendly as well as cost efficient. This paper aims in the study of various dynamic properties of cellular lightweight concrete. The dynamic properties with different strain rate can be studied using Split Hoopkins Pressure Bar (SHPB). Dynamic compressive strength increases with strain. Impact and toughness of lightweight cellular concrete also increases with strain rate under impact loading.*

Key Words: Cellular lightweight concrete, strength, dynamic, strain rate, impact, toughness.

1. INTRODUCTION

Cellular Lightweight Concrete is manufactured by mixing Portland cement, sand, fly ash, water and performed foam in varied proportions. The air content is maintained between 40-80% of the total volume. The amount of foaming agent added to the concrete mixture will determine the amount of air trapped in, which can range from 10% to 70%. The density of CLC ranges between 400 and 1800 Kg/m^3. The ratio of the foam to the neat cement slurry controls the unit weight of the lightweight cellular concrete CLC reduces the self-weight of the structure which minimizes the dimensions of the structural members. CLC can be used as thermal insulation in the form of bricks and blocks, bulk filling for old sewer pipes walls unused cellar and basements storage tanks etc. Main applications are as backfill of retaining wall lightweight pavements, landslip repairs, bridge approach and to provide shock absorption urges us to find its response to dynamic loads.

2. TEST METHODS

2.1 Split Hoopkins Pressure Bar

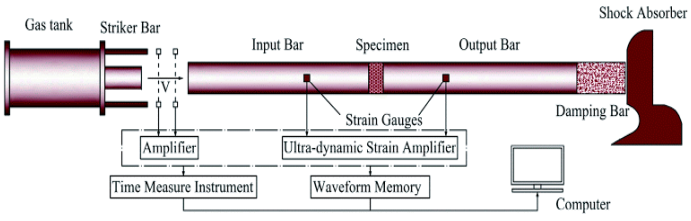

Fig-1: 100 mm-diameter SHPB apparatus

Er-Le-Bai et al, (2018). The apparatus consists of main body, energy source and measurement systems. The length of projectile is 500mm, diameter of compression bar is 100mm. The basic principle of SHPB is propagation theory of elastic stress waves on the bar. The test is based on two assumptions 1) plane assumption: in the propagation process, each cross-section of elastic bars is always kept in plane state 2) equal stress assumption: stress in specimen is equal everywhere.

Er-Le-Bai et al, (2018). The specimen is placed between the input and the output bars. When the striker bar is pulsed by high pressure gas from the tank it strikes the input bar and for an elastic stress wave which then spreads through the input bar. On reaching the interface between the input bar and the specimen, some wave passes though the interface to reach the specimen while the rest gets reflected back into the input bar. The same process takes place at the interface between output and specimen. This process is continued until it reaches a state of equilibrium.

Changchun Shi et al, (2017). For comparative study concrete specimens with densities of 360 kg/m^3, 570 kg/m^3, 820kg/m^3 are considered.

2.2 Cyclic Simple Shear Testing

It is an automated computer-controlled apparatus which uses a stack of 31 Teflon rings each 0.94mm thick which confine the specimen laterally. A servo-motor is used to apply the horizontal loads and a micro-stepper is used to apply vertical loads.

Binod Tiwari et al, (2018). The specimens are placed on the rubber membrane confined by the sack of Teflon rings and secured in the apparatus. The computer connected to the device displays the real time logarithm of time versus displacement curves which are used to determine the end of primary consolidation.

At this point the cyclic loading phase begins. Chat-1 represents the cyclic loading function. These cyclic loading contains a series of sinusoidal waves with a frequency of 0.5 Hz. The sinusoidal waves had double amplitude shear strain values of 0.08, 0.10, 0.12, 0.14, 0.16, 0.18, 0.20, 0.30, 0.40, 0.50, 0.60, 0.70, 0.80, 0.90, and 1.00%.

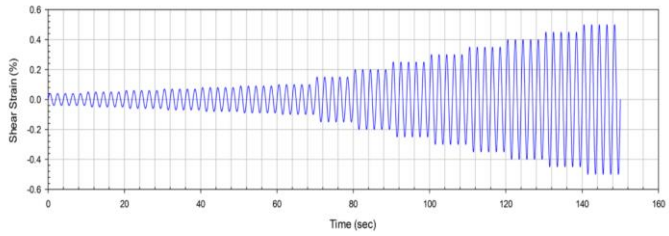

Chart-1: . Cyclic loading function used in the cyclic simple shear tests conducted

3. DYAMIC PROPERTIES

3.1 Stress-strain curve

Changchun Shi et al, (2017) The nominal stress strain curve for CLC with three different densities are illustrated in Chart-2. Nominal stress-strain refers to the stress and strain that are not taken into account for the geometric discontinuity of the mater

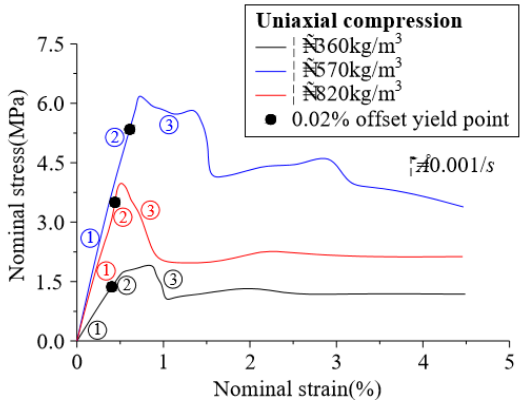

Chart-2: Nominal stress-strain curves of CLC with three different densities

At the initial stages of material compression, the stress-strain curves show a linear and rapid growth trend, stress reaches its peak value for a small rate of strain. Microcracks appear on the material at this stage and stress concentration begins to appear in local areas. When the local stress is greater than the breaking strength of the material, macro-cracks appear in the concrete and lead to brittle fracture. At this moment, the nominal stress-strain curve of the material suddenly to a certain point and the curve gradually stabilizes, but it does not reach 0, this shows that there is no instantaneous failure when the pressure exceeds its ultimate compressive strength and there is still some bearing capacity left.

The second stage which is the platform stage is where energy is absorbed by the concrete. The stresses are decreased significantly at this stage, and then the stress continuously oscillates at a low level, which indicates that there are both strain-hardening as well as strain-softening behaviors in this stage. Macro appears at this stage which causes surface spalling. Towards the end of this stage most of the cells are destroyed and the cell walls touch and rub with each other and the external load is borne by the deformation of concrete mass. During the densification stage the stress-strain curve shows a rebound. Greater the density of concrete earlier will be the densification stage.

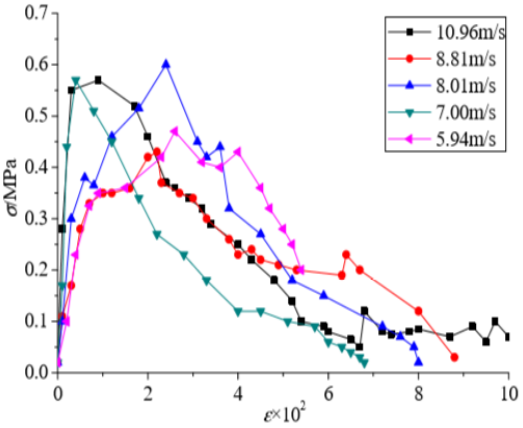

Chart-3: Dynamic stress-strain curves at different impact velocities

From Chart- 3 it is inferred that the dynamic strength of CLC is small.

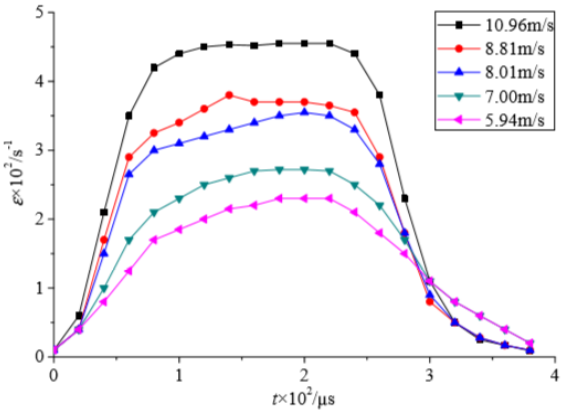

Chart-4: Strain rate curves at different impact velocities

As from Chart-4 it can be seen that the strain rate and impact velocity in concrete show a positive correlation.

3.1.1 Strength Properties

Er-Le-Bai et al, (2018) The dynamic compressive strength is defined as the peak stress in the dynamic compression curve and is one of the major indicator that reflects the dynamic strength of the material.

From chart-6 It can be seen that the dynamic compression strength increases with an increase in strain rate.

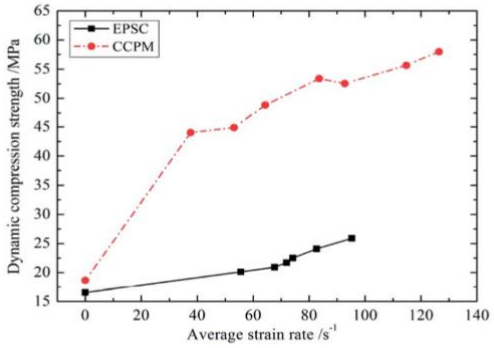

Chart-5: Relationship between dynamic compression strength and strain rate of two different types of CLC materials.

3.1.2 Impact toughness

Er-Le-Bai et al, (2018). Impact toughness can be usually expressed by the area enclosed by the stress-strain curve and axial strain. From Cart-6 it can be concluded that impact toughness of CLC increases with strain rate.

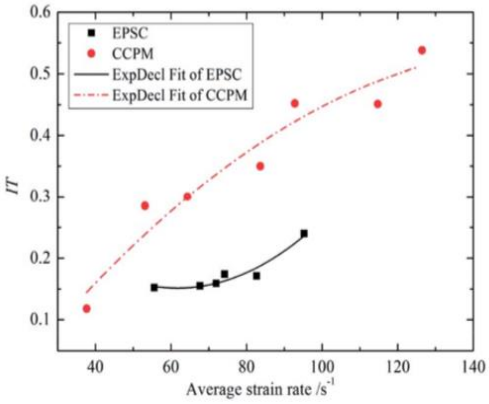

Chart-6: The relationship between Impact Toughness and strain rate.

3.2. Stress-Strain Hysteresis Loop

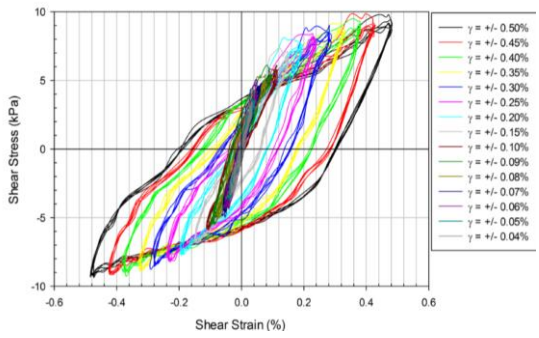

Chart-7: Hysteresis loops from the cyclic simple shear

Binod Tiwari et al, (2018). From Chart-7 As the amplitude of the cyclic loading function the area enclosed in the hysteresis loop reduces with shear strain Decrease in consolidation pressure can also cause a reduction in the enclosed area. These hysteresis loops can be used to develop backbone curve for CLC.

3.3 Backbone Curves

Binod Tiwari et al, (2018) Chart-8 indicates the backbone curve obtained from hysteresis loop obtained by fitting the hyperbolic function Eq (1) where σ_v' is in KPa,

$$\tau = \frac{a\gamma}{b+\gamma} \quad (1)$$

$$a = 0.4593\sigma_v' \quad (2)$$

$$b = 0.0027\sigma_v' + 0.0502 \quad (3)$$

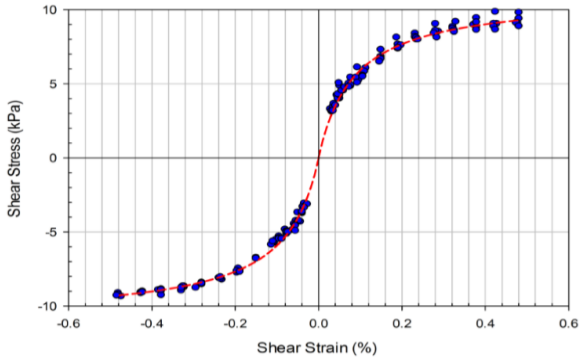

Chart-8: Backbone curve obtained from the hysteresis loops

Where τ is the shear stress, γ is the shear strain, and a and b are curve-fitting parameters. The data points represent the peaks and troughs, corresponding to the points of stress reversal in the stress-strain hysteresis loops from Chart-7

An increase in the consolidation pressure resulted in an upward shift of the backbone curve.

3.4 Maximum Shear Modulus (G_{max})

Binod Tiwari et al, (2018) . The maximum shear modulus can be calculated by taking the derivative of the hyperbolic function and then calculating the value of the resulting function at a shear strain of zero

From chart-9 it is clear that the maximum shear modulus increase as the consolidation pressure increases, but the rate of increase in the maximum shear modulus with the consolidation pressure appears to be similar. The maximum shear modulus decrease as the unit weight of the CLC test specimen's increases.

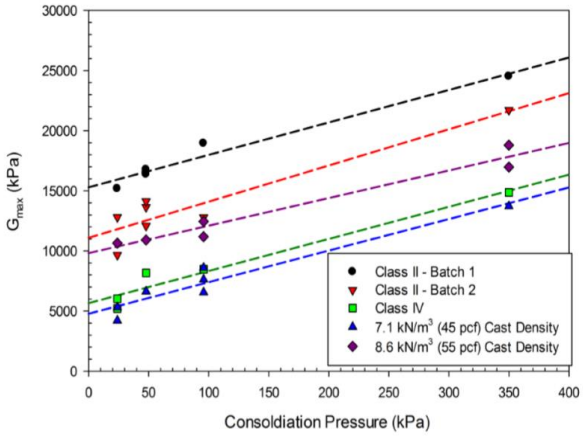

Chart-9: Relationship between the maximum shear modulus and the consolidation pressure for CLC specimens with different unit weights

3.5 Modulus Reduction Curve

Binod Tiwari et al, (2018) Chart-10 contains a typical set of modulus reduction curves for CLC samples. At a constant shear strain, the ratio of the shear modulus to the maximum shear modulus ($G=G_{max}$) decreased as the consolidation pressure increased

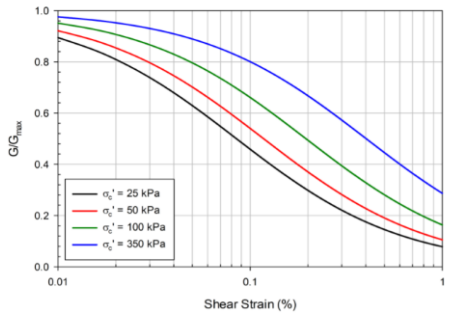

Chart- 10 : Modulus reduction curves for CLC specimens consolidated to different vertical stresses

3.6. Damping Ratio

Binod Tiwari et al, (2018). Damping ratio is a dimensionless measure which describes about how the oscillations in a system decay after disturbance. The damping ratio depends on the unit weight of the CLC specimens. From Chart- 11 it is perspicuous that the damping ratio depends on both the consolidation pressure and the shear strain. Besides the sample consolidated to an effective stress of 25KPa, increase in the shear strain resulted in a slight decrease in the damping ratio between the shear strains of 0.25 and 0.35%, beyond this shear strain values, there is a significant increase in damping ratio with an increase in shear strain. The shear strain values corresponding to when the change in the mode of damping occurred depends on the consolidation pressure.

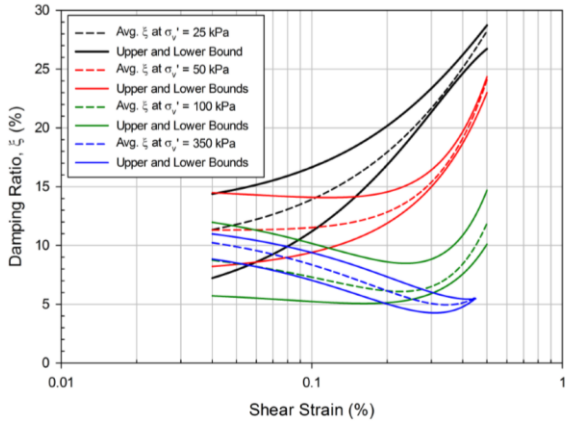

Chart-11: Relationship between the damping ratio, the shear strain and the consolidation pressure

3.7 Energy Dissipation Analysis

Yuan Pu, Ma Qinyong, Zhang Haidong (2014). The sample is tested using an Aluminum Modified Split Hoopkins Pressure Bar Apparatus, where the length of striker bar is 0.60 m. The incident pulse energy W_i, reflected pulse energy W_r, transmitted pulse energy W_t and absorbing energy of specimen W_s.

Yuan Pu, Ma Qinyong, Zhang Haidong (2014). Energy absorbing property of foamed concrete mainly comes from its long "plateau regime" of the three-regime stress-strain curve. The absorbing energy of light-weight foam concrete in impact compression test can be calculated as :$WS=W_i - W_r - W_t$

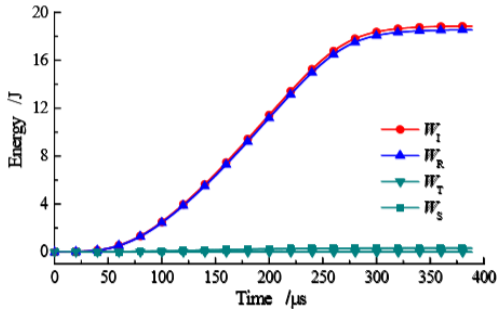

Chart-12: Energy *versus* time curve

Chart-12 shows a time resolved energies involved in impact compression test when striker velocity is 5.90 m/s. it is noticeable from the chart that the time resolved energy for incident wave increases with the time growing at the initial phase and after reaching a certain value they attain a constant value. The reflected wave also ends to follow the same pattern. The transmitted energy and energy absorbed by light-weight foam concrete is much small. The reflected wave energy is slight less than incident wave energy. Therefor it can be inferred that only a few energies pass

through the specimen to reach the output bar most of the incident energy is reflected back into the input bar. EAR decreases as the incident wave energy W_i increasing in a negative power relation approach. In the initial phase EAR decreases in a fast rate, then becomes constant after reaching a certain point. Another scatter diagram is drawn in a similar way with striker velocity on x-axis and EAR on the y-axis as shown in chat 13 b). EAR decreases as the striker velocity v increases.

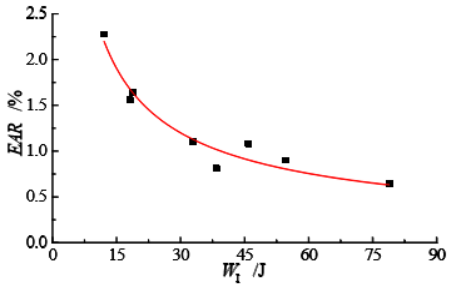

a)

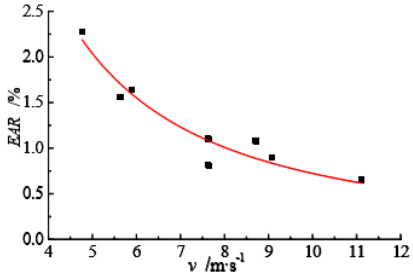

b)

Chart-13: Curve of EAR vs W_i

3.8 Shrinkage Deformation in CLC

A I Kudyakov and A B Steshenko (2015). The primary cause of shrinkage deformation of foam concrete of natural hardening are cracks occurring in concrete's interporous partition walls during the technological processing of raw materials and hardening of the cement stone. The energy of any loaded volume is converted into crack and leads to the destruction of the material.

Raj Vardhan Singh Chandel, Rashmi Sakale (2016) Due to the intensive percolation of wall pores it causes the pores to combine to form larger pores which increases the shrinkage and causes the deterioration of its operational properties. A significant decrease in the values of shrinkage strain of the foam concrete during the natural hardening can predict a reduced level of stresses formation in the structure of foam concrete. Shrinkage deformation of CLC occurs due to cracks occurring in concrete's interporous partition walls.

4. CONCLUSIONS

The shape of the backbone curve depended significantly on effective normal stress. The maximum shear modulus increased with a decrease in unit weight of the CLC material and an increase in the effective normal stress. Reduction in the shear modulus with the shear strain also depends on the effective normal stress. The damping ratio which decreases with increasing shear strain for shear strains less than 0.25% to 0.35%. On the other hand, for shear strains greater than 0.25% to 0.35%, the damping ratio increases with an increase in the shear strain.

The reflected wave energy W_r as from SHPB test is in same order of magnitude with incident wave energy WI and their values are almost the same. Energy absorption rate EAR of CLC decreases with incident wave energy W_i. There is also a similar relation between Energy absorption rate EAR and striker velocity v. The whole process of uniaxial compression of foam concrete is divided into three stages, namely the material's elastic and plastic stage, the platform stage, and the material densification stage.

REFERENCES

[1] Binod Tiwari, Beena Ajmera, Diego Villegas (2018): Dynamic properties of lightweight cellular concrete for geotechnical applications. ASCE journal of materials in civil engineering Vol 30 (2)

[2] Changchun Shi, Xinghai Song, Chengjie Wang (2017): study on Quasi static and Dynamic mechanical properties of chemical foaming concrete. Chemical engineering transactions Vol 6.

[3] Er-Lei bai, Jin-Yu Xu, Song Lu, Ke-Xin Lin and Yi-Ming Zhang (2018); Comparative study on the dynamic properties of lightweight porous concrete. The Royal Society of Chemistry (26).

[4] Raj Vardhan Singh Chandel, Rashmi Sakale (2016); study of cellular lightweight concrete. International Journal for scientific research & development Vol 4, (07).

[5] Yuan Pu, Ma Qinyong, Zhang Haidong (2014); Energy Dissipation Analyses on Lightweight Foam Concrete under Impact Loads. Electronic Journal of Geotechnical Engineering Vol 19.

[6] A I Kudyakov and A B Steshenko (2015), ''Shrinkage deformation of cement foam concrete''. Proceedings of IOP Conf. Series: Materials Science and Engineering 71 in Tomsk, Russia.